Journal of the Chinese Institute of Engineers, Vol. 22, No. 6, pp. 741-751 (1999)

FRACTURE PROPAGATION OF ANISOTROPIC PLATES BY THE BOUNDARY ELEMENT METHOD

Chao-Shi Chen* and Chien-Chung Ke
Department of Resource Engineering
National Cheng Kung University
Tainan, Taiwan 701, R.O.C.

Key Words: boundary element method, stress intensity factor, fracture propagation, anisotropic elasticity

ABSTRACT

This paper presents a boundary element method combined with the maximum tensile stress criterion for predicting crack initiation angles and simulating fracture propagation paths in cracked anisotropic plates under mixed mode loading. Since the calculated displacements near the crack tip by the BEM have been verified to be very accurate, a decoupling technique can be used to determine the mixed mode stress intensity factors based on the definition of the J-integral and the relative displacements at the crack tip. Numerical examples are presented for the calculation of stress intensity factors for both isotropic and anisotropic cases. It can be found that our numerical results are in good agreement with those reported by previous authors. Fracture propagation in an anisotropic plate under mixed mode loading is simulated by an incremental crack extension with a piece-wise linear discretization. A computer program, which can automatically generate a new mesh (required for analyzing sequentially the boundary configuration) has been developed to simulate the fracture propagation process. It was found that the numerical analysis could predict relatively well the direction of crack initiation and the path of fracture propagation.

I. INTRODUCTION

Fracture mechanics is essentially based on the extension of Griffith theory (1920) and Irwin's modification (1957) to that theory which recognizes the importance of stress intensity near the end of a crack tip. Irwin (1957) introduced parameters, called stress intensity factors (SIF's), to express the stress and displacement fields near a crack tip. In general, three SIF's, called K_I, K_{II}, and K_{III}, are introduced, corresponding to three basic fracture modes, e.g. mode I (opening mode), mode II (sliding mode) and Mode III (tearing mode), respectively. A superposition of the three modes describes the general case of loading (mixed mode loading). For a given cracked body under a certain type of loading, the SIF's are known and the stresses and displacements near the crack tip can, accordingly, be determined. Hence, the problem of linear elastic fracture mechanics reduces to the determination of the crack tip SIF's. The methods, which are commonly employed in the determination of the SIF's can be generally divided into three categories (Whittaker *et al.*, 1992): (1) analytical methods, including the complex stress functions, weight functions, and stress concentration methods; (2) numerical methods, including the finite element

*Correspondence addressee

method (FEM), boundary element method (BEM), finite difference method (FDF), and boundary collocation method (BCM); and (3) experimental methods, including the commonly used photoelastic techniques, acoustics and indirect measurements such as compliance calibration from laboratory tests.

In this paper, the BEM was selected for the analysis of crack initiation and propagation of anisotropic cracked plates. Fracture propagation processes are frequently simulated by an incremental crack extension analysis, based on certain failure criteria to predict the direction of crack initiation. For each increment of crack extension, a stress analysis is carried out and the SIF's are evaluated. Because of the complex geometry, which is continuously changing during crack extension, numerical techniques are required to simulate crack propagation problems. For a long time, the FEM has been used to determine the SIF's for cracked media. Numerous researchers have employed this method to study fracture propagation processes (Shephard *et al.*, 1985; Boone *et al.*, 1987; Wawrzynek *et al.*, 1988; Swenson and Ingraffea, 1988; Wei and De Bremaecker, 1994). The main disadvantage of the FEM in dealing with this problem is that the finite element mesh has to be updated following each step of crack extension.

The BEM has been proven to be a powerful numerical technique with certain advantages over the domain-based method such as the FEM. Over the past ten years, the BEM has emerged as an alternative method for the analysis of cracked bodies (Chen and Hong, 1992). However, because the coincidence of the crack surfaces gives rise to a singular system of algebraic equations, the solution of this problem can not be obtained with the direct formulation of the BEM. Some special techniques have been devised to overcome this difficulty such as the Green's function method (Snyder and Cruse, 1975), the sub-regional method (Blandford *et al.*, 1981; Sollero *et al.*, 1994; Sollero and Aliabadi, 1995), the displacement discontinuity method (DDM) (Crouch and Starfield, 1983; Shen and Stephansson, 1994; Scavia, 1995). The Green's function method has the advantages of avoiding crack surface modeling and gives excellent accuracy. It is however, restricted to very simple crack geometry for which analytical Green's functions are available. The sub-regional method introduces artificial boundaries into several sub-regions, thus resulting in a large system of equations. In fracture propagation analysis, these artificial boundaries must be repeatedly introduced for each increment of crack extension. Hence, this method can not be easily implemented as an automatic procedure in an incremental analysis of crack extension problems (Portela *et al.*, 1993). The main disadvantage of the DDM is that the kernel functions in DDM involve singularities with orders higher than those in the traditional displacement BEM. Hence, this method is not suitable for problems involving finite domains.

In recent years, the single-domain BEM has been proposed for the study of cracked media (Hong and Chen, 1988; Gray *et al.*, 1990; Portela *et al.*, 1992; Sollero and Aliabadi, 1995; Pan and Amadei, 1996; Pan, 1997; Aliabadi, 1997; Chen and Hong, 1999). It involves two sets of boundary integral equations and is, in general, superior to the aforementioned BEM's. As a consequence, general mixed mode crack problems can be solved in a single-domain BEM formulation. The single-domain analysis can eliminate remeshing problems, which are typical of the FEM and the sub-regional BEM. The single-domain BEM has received considerable attention and has been found to be a good method for simulating crack propagation processes.

In this paper, the single-domain BEM formulation combined with the maximum tensile stress criterion were used to predict the angle of crack initiation and to simulate the path of fracture propagation in anisotropic plates. The BEM formulation is such that the displacement integral equation is collocated on the outside boundary only and the traction integral equation on one side of the crack surface only. A decoupling technique can be used to determine the mixed mode SIF's based on the definition of the J-integral and the relative displacements at the crack tip. Numerical examples are presented for the calculation of mixed mode SIF's for both isotropic and anisotropic cases. It can be found that our numerical results are in good agreement with those reported by previous authors. Fracture propagation in an anisotropic homogeneous plate under mixed mode I-II loading is simulated by an incremental crack extension with a piece-wise linear discretization. A computer program, which can automatically generate a new mesh (required for analyzing, sequentially, the changing boundary configuration) has been developed to simulate the fracture propagation process. Some experimental observations of crack initiation angles and fracture propagation were obtained by conducting diametrical loading of circular cracked disc specimens of a bedding oil shale. It was found that the numerical analysis could predict relatively well the path of fracture propagation.

II. THEORETICAL BACKGROUND

1. Anisotropic Elasticity

As shown in Lekhnitskii (1957), the stress and displacement fields in a two-dimensional linear elastic, homogeneous, and anisotropic medium can be formulated in terms of two analytical functions,

$\phi_k(z_k)$, of the complex variables $z_k=x+\mu_k y$ (k=1, 2), where μ_k are the roots of the following characteristic equation

$$a_{11}\mu^4-2a_{16}\mu^3+(2a_{12}+a_{66})\mu^2-2a_{26}\mu+a_{22}=0. \quad (1)$$

In Eq. (1), a_{11}, a_{12}, ..., a_{66} are the compliance components of the medium in a global coordinate system (x, y) attached to the medium. The detailed relation of these components with the material elasticity can be found in Chen *et al.* (1998). Lekhnitskii has shown that the roots of Eq. (1) are always either complex or purely imaginary, two of them being the conjugate of the two others. Let μ_1, μ_2 be those roots and $\overline{\mu_1}$, $\overline{\mu_2}$ their respective conjugates. Assuming μ_1 and μ_2 to be distinct, the general expressions for the stress and displacements are (Lekhnitskii , 1957; Sih *et al.*, 1965)

$$\sigma_x=2\mathrm{Re}[\mu_1^2\phi_1'(z_1)+\mu_2^2\phi_2'(z_2)]$$

$$\sigma_y=2\mathrm{Re}[\phi_1'(z_1)+\phi_2'(z_2)]$$

$$\tau_{xy}=-2\mathrm{Re}[\mu_1\phi_1'(z_1)+\mu_2\phi_2'(z_2)] \quad (2)$$

and

$$u=2\mathrm{Re}[P_{11}\phi_1(z_1)+P_{12}\phi_2(z_2)]$$

$$v=2\mathrm{Re}[P_{21}\phi_1(z_1)+P_{22}\phi_2(z_2)], \quad (3)$$

where

$$P_{1k}=a_{11}\mu_k^2+a_{12}-a_{16}\mu_k$$

$$P_{2k}=a_{12}\mu_k+a_{22}/\mu_k-a_{26}. \ (k=1, 2) \quad (4)$$

2. BEM Formulation for Determining SIF's

For concentrated point forces acting at z_k^0 ($z_k^0=x^0+\mu_k y^0$) in an infinite plate, the Green's tractions, T_{ij}, and displacements, U_{ij}, are equal to (Sollero and Aliabadi, 1993)

$$T_{ij}(z_k, z_k^0)=2\mathrm{Re}[Q_{j1}(\mu_1 n_x-n_y)A_{i1}/(z_1-z_1^0)$$
$$+Q_{j2}(\mu_2 n_x-n_y)A_{i2}/(z_2-z_2^0)] \quad (5)$$

and

$$U_{ij}(z_k, z_k^0)=2\mathrm{Re}[P_{j1}A_{i1}\ln(z_1-z_1^0)$$
$$+P_{j2}A_{i2}\ln(z_1-z_2^0)]. \ (i, j=1, 2) \quad (6)$$

In Eqs. (5) and (6), n_x and n_y are the outward normal vectors of the field point, and $Q_{11}=\mu_1$, $Q_{12}=\mu_2$, and $Q_{21}=Q_{22}=-1$. The complex coefficients A_{jk} are solutions of the following equation

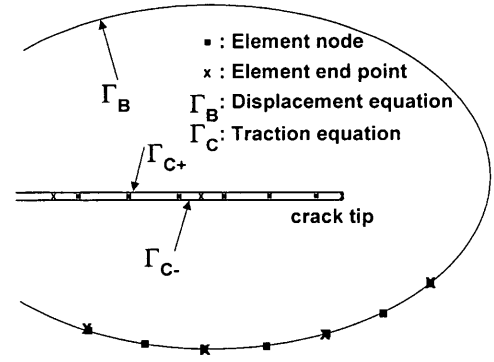

Fig. 1. Geometry of a two-dimensional cracked domain.

$$\begin{bmatrix} 1 & -1 & 1 & -1 \\ \mu_1 & -\overline{\mu_1} & \mu_2 & -\overline{\mu_2} \\ P_{11} & -\overline{P_{11}} & P_{12} & -\overline{P_{12}} \\ P_{21} & -\overline{P_{21}} & P_{22} & -\overline{P_{22}} \end{bmatrix} \begin{bmatrix} A_{j1} \\ \overline{A_{j1}} \\ A_{j2} \\ \overline{A_{j2}} \end{bmatrix} = \begin{bmatrix} \delta_{j2}/(2\pi i) \\ -\delta_{j1}/(2\pi i) \\ 0 \\ 0 \end{bmatrix} \quad (7)$$

where δ_{jk} is the Kronecker's delta.

The traditional displacement boundary integral equation for linear elasticity can be expressed as

$$c_{ij}(z_k^0)u_j(z_k^0)+\int_\Gamma T_{ij}(z_k, z_k^0)u_j(z_k)d\Gamma(z_k)$$
$$=\int_\Gamma U_{ij}(z_k, z_k^0)t_j(z_k)d\Gamma(z_k) \quad (8)$$

where i, j, k=1, 2; T_{ij} and U_{ij} are the Green's tractions and displacements given in Eqs. (5) and (6); u_j and t_j are the boundary displacements and tractions; c_{ij} are quantities that depend on the geometry of the boundary and are equal to $\delta_{ij}/2$ for a smooth boundary; and z_k and z_k^0 are the field and source points on the boundary Γ of the domain. Discretization of Eq. (8) gives a linear system of algebraic equations which can be solved for the unknowns on the boundary. However, for a cracked elastic medium, Eq. (8) is not sufficient for solving all the unknowns along the outer boundary of the problem as well as along the two sides of the crack surfaces because of the geometric singularity associated with the crack surface.

For cracked anisotropic media, the displacement integral equation is collocated on the outer boundary only and the traction integral equation on one side of the crack only (Pan and Amadei, 1996). The displacement integral Eq. applied to the outer boundary results in the following form ($z_{k,B}^0 \in \Gamma_B$ only, Fig. 1)

$$c_{ij}(z^0_{k,B})u_j(z^0_{k,B}) + \int_{\Gamma B} T_{ij}(z_{k,B}, z^0_{k,B})u_j(z_{k,B})d\Gamma(z_{k,B})$$

$$+ \int_{\Gamma C} T_{ij}(z_{k,C}, z^0_{k,B})[u_j(z_{k,C+}) - u_j(z_{k,C-})]d\Gamma(z_{k,C})$$

$$= \int_{\Gamma B} U_{ij}(z_{k,B}, z^0_{k,B})t_j(z_{k,B})d\Gamma(z_{k,B}) \qquad (9)$$

where Γ_C has the same outward normal as Γ_{C+}. Here, the subscripts B and C denote the outer boundary and the crack surface, respectively.

The traction integral equation (for z^0_k being a smooth point on the crack) applied to one side of the crack surfaces is ($z^0_{k,C} \in \Gamma_{C+}$ only)

$$0.5t_l(z^0_{k,C}) + n_m(z^0_{k,C})\int_{\Gamma B} c_{lmik}T_{ij,k}(z^0_{k,B}, z_{k,B})u_j(z_{k,B})d\Gamma(z_{k,B})$$

$$+n_m(z^0_{k,C})\int_{\Gamma C} c_{lmik}T_{ij,k}(z^0_{k,C}, z_{k,C})[u_j(z_{k,C+}) - u_j(z_{k,C-})]d\Gamma(z_{k,C})$$

$$= n_m(z^0_{k,C})\int_{\Gamma B} c_{lmik}U_{ij,k}(z^0_{k,C}, z_{k,B})t_j(z_{k,B})d\Gamma(z_{k,B}) \qquad (10)$$

where n_m is the unit outward normal to the contour path; and the gradient tensors $T_{ij,k}$ and $U_{ij,k}$ denote differentiation with respect to z^0_k.

The Cauchy singularity in the displacement Eq. (9) can be avoided by the rigid-body motion method. The integrand on the right-hand side of Eq. (9) has only integrable singularity, which can be resolved by the bi-cubic transformation method (Cerrolaza and Alarcon, 1989). The traction Eq. (10) involves a Hadamard finite-part integral. For isotropic materials with a piece-wise flat crack assumption, the integral can be carried out by direct analytical integration (Portela *et al.*, 1992). For anisotropic media, however, the integral is very complicated and its analytical evaluation is almost impossible. Although different methods have been suggested to deal with such integrals (Portela *et al.*, 1992; Hildenbrand and Kuhn, 1993; Linkov and Mogilevskaya, 1994), they usually require the evaluation of a limit value of the integrand at the singular point, which is possible only for the case where the integrand has a simple and exact closed form expression. In this paper, the finite-part integral is resolved by the Gauss quadrature formula which is very similar to the traditional weighted Gauss quadrature but with a different weight. Details of the Gauss quadrature formula can be found in the papers of Tsamasphyros and Dimou (1990) and Pan and Amadei (1996). Therefore, Eqs. (9) and (10) can be solved simultaneously for the unknown displacements or tractions on the outer boundary, and the unknown crack displacement differences on the crack surface.

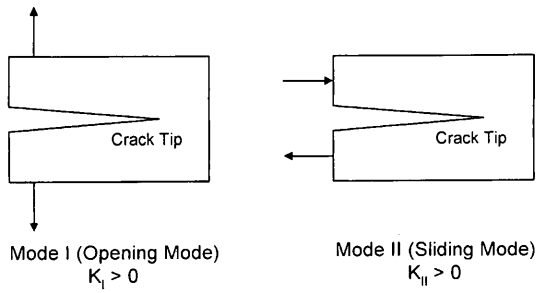

Fig. 2. Sign convention used for determining SIF's in mode I and mode II.

In this study, the discontinuous quadratic elements were used to discretize the crack boundary (Fig. 1). The node positions for this kind of elements are s=−2/3, 0, 2/3. In order to capture the square-root characteristics of the relative crack displacements near the crack tip, the following crack tip element with its tip at s=−1 was employed

$$u_i = \sum_{k=1}^{3} \phi_k u_i^k, \qquad (11)$$

where the subscript i (=1, 2, 3) denotes the components of the relative crack displacement, and the superscript k (=1, 2, 3) denotes the displacements at nodes, respectively. The shape functions ϕ_k are (Pan and Amadei, 1996)

$$\phi_1 = [\frac{5}{3} - \sqrt{\frac{5}{3}} - \frac{2}{3}\sqrt{s+1} + (\sqrt{\frac{5}{3}} - 1)(s+1)]/\Delta$$

$$\phi_2 = [\frac{1}{3} - \sqrt{\frac{5}{3}} - \frac{5}{3}\sqrt{\frac{1}{3}} + \frac{4}{3}\sqrt{s+1} + (\sqrt{\frac{1}{3}} - \sqrt{\frac{5}{3}})(s+1)]/\Delta$$

$$\phi_3 = [\sqrt{\frac{1}{3}} - \frac{1}{3} - \frac{2}{3}\sqrt{s+1} + (1 - \sqrt{\frac{1}{3}})(s+1)]/\Delta$$

$$\Delta = \frac{2}{3}(2 - \sqrt{\frac{1}{3}} - \sqrt{\frac{5}{3}}) \qquad (12)$$

The mixed mode SIF's for anisotropic media can be determined by using the J-integral combined with a decoupling technique (Sollero and Aliabadi, 1993). This technique is based on the ratio of relative crack tip displacements calculated with the BEM. The mode II SIF, K_{II}, can be determined by

$$K_{II} = \sqrt{\frac{J_1}{\alpha_{11}\rho^2 + \alpha_{12}\rho + \alpha_{22}}}, \qquad (13)$$

where J_1 is the J-integral related to K_I, α_{ij} are constants related to the elastic properties of the anisotropic medium, and ρ, is the ratio of K_I to K_{II}. Once K_{II} is calculated from Eq. (13), K_I=ρK_{II}. In this paper, the sign convention for the corresponding SIF's (K_I and K_{II}) is shown in Fig. 2.

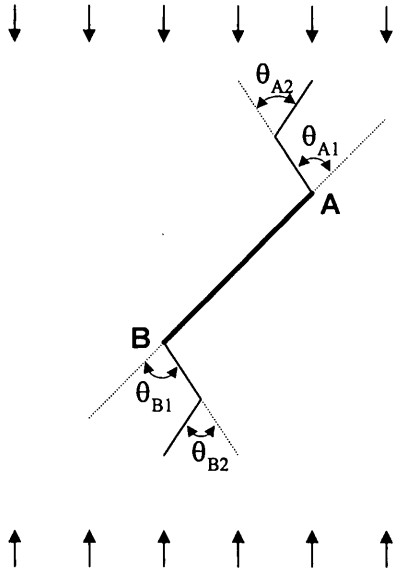

Fig. 3. Process of crack propagation by increasing linear elements.

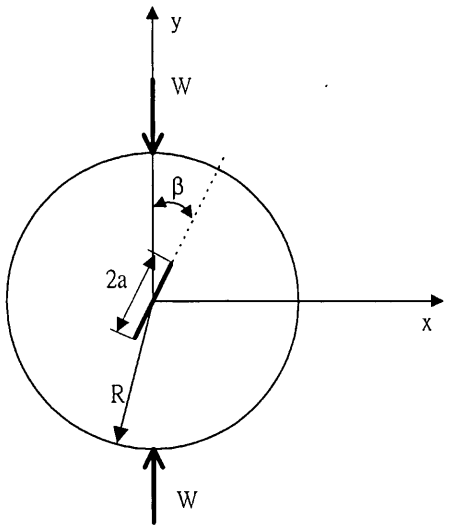

Fig. 4. An isotropic circular plate with a central crack subjected to concentrated diametrical loading.

3. Crack Initiation and Fracture Propagation

In fracture mechanics, there are three criteria commonly used to predict the crack initiation angle: the maximum tensile stress criterion, or σ-criterion (Erdogan and Sih, 1963); the maximum energy release rate criterion, or G-criterion (Palaniswamy and Knauss, 1972); and the minimum strain energy density criterion, or S-criterion (Sih, 1974). Among them, the σ-criterion has been found to predict well the directions of crack initiation compared to the experimental results for polymethylmethacrylate (Woo and Ling, 1984; Richard, 1984) and for brittle clay (Vallejo, 1987). Because of its simplicity, the σ-criterion seems to be the most popular criterion in mixed mode I-II fracture studies (Whittaker *et al.*, 1992). Therefore, the σ-criterion was used in this study to determine the crack initiation angle for anisotropic plates. For the σ-criterion, the angle of crack initiation, θ_0, must satisfy

$$\frac{\partial \sigma_\theta}{\partial \theta} = 0 \text{ (or } \tau_{r\theta}=0) \text{ and } \frac{\partial^2 \sigma_\theta}{\partial \theta^2} < 0, \qquad (14)$$

where σ_θ and $\tau_{r\theta}$ are normal and shear stresses in the polar coordinates (r and θ). A numerical procedure was applied to find the angle θ_0 when σ_θ is a maximum for known values of the material elastic constants, the anisotropic orientation angle ψ, and the crack geometry.

In this paper, the real process of crack propagation in an anisotropic plate under mixed mode I-II loading is simulated by incremental crack extension with a piece-wise linear discretization. For each incremental analysis, crack extension is conveniently modeled by a new boundary element. A computer program has been developed to automatically generate new data required for analyzing, sequentially, the changing boundary configuration. Based on the calculation of the SIF's and crack initiation angle for each increment, the procedure of crack propagation can be simulated. The steps in the crack propagation process are summarized as follows (Fig. 3):

(1) Compute the SIF's using the proposed BEM;
(2) Determine the angle of crack initiation based on the maximum tensile stress criterion;
(3) Extend the crack by a linear element (of length selected by the user) along the direction determined in step 2;
(4) Automatically generate the new BEM mesh;
(5) Repeat all the above steps until the new crack is near the outer boundary.

III. NUMERICAL EXAMPLES OF SIF's

Two numerical examples including isotropic and anisotropic plates were selected to test our BEM program for determining SIF's. A generalized plane stress deformation is assumed in all examples. The first example analyzed here is that of an isotropic thin circular plate of radius R and thickness t with a central crack of length $2a$ loaded by a pair of concentrated and diametrical compressive loads, W (Fig. 4). The outer boundary and the crack surface are discretized with 28 continuous and 10 discontinuous quadratic elements, respectively. Two cases are analyzed: (1) a/R=0.5, the crack angle β varies between 0 and $\pi/2$, and (2) β=45°, a/R varies between 0.1 and 0.7. The two normalized SIF's, $K_I/\sigma\sqrt{\pi a}$ and $K_{II}/\sigma\sqrt{\pi a}$ where $\sigma=W/\pi Rt$, calculated with the BEM program for these two cases, are compared with those obtained by Atkinson *et al.* (1982), using the

Table 1. Normalized SIF's for a Central Slant Crack in an Isotropic Circular Plate Subjected to a Concentrated Load (a/R=0.5).

β	Atkinson *et al.* (1982)		This study	
(Rad.)	$K_I/\sigma\sqrt{\pi a}$	$K_{II}/\sigma\sqrt{\pi a}$	$K_I/\sigma\sqrt{\pi a}$	$K_{II}/\sigma\sqrt{\pi a}$
0	1.387	0	1.339	0
$\pi/16$	0.970	-1.340	0.960	-1.275
$2\pi/16$	0.030	-2.113	0.074	-2.061
$3\pi/16$	-0.946	-2.300	-0.903	-2.275
$\pi/4$	-1.784	-2.132	-1.737	-2.103
$5\pi/16$	-2.446	-1.728	-2.377	-1.711
$6\pi/16$	-2.885	-1.188	-2.826	-1.197
$7\pi/16$	-3.127	-0.604	-3.092	-0.614
$\pi/2$	-3.208	0	-3.180	0

Table 2. Normalized SIF's for a Central Slant Crack in an Isotropic Circular Plate Subjected to a Concentrated Load (β= 45°).

a/R	Atkinson *et al.* (1982)		This study	
	$K_I/\sigma\sqrt{\pi a}$	$K_{II}/\sigma\sqrt{\pi a}$	$K_I/\sigma\sqrt{\pi a}$	$K_{II}/\sigma\sqrt{\pi a}$
0.1	-1.035	-2.010	-1.020	-1.968
0.2	-1.139	-2.035	-1.116	-1.995
0.3	-1.306	-2.069	-1.272	-2.036
0.4	-1.528	-2.100	-1.484	-2.069
0.5	-1.784	-2.132	-1.737	-2.103
0.6	-2.048	-2.200	-2.020	-2.148
0.7	–	–	-2.337	-2.213

Table 3. Normalized SIF's for a Central Inclined Crack in an Anisotropic Rectangular Plate Subjected to a Uniform Tension.

ψ	Gandhi (1972)		Sollero and Aliabadi (1993)		This study	
(Deg.)	$K_I/\sigma\sqrt{\pi a}$	$K_{II}/\sigma\sqrt{\pi a}$	$K_I/\sigma\sqrt{\pi a}$	$K_{II}/\sigma\sqrt{\pi a}$	$K_I/\sigma\sqrt{\pi a}$	$K_{II}/\sigma\sqrt{\pi a}$
0	0.522	0.507	0.510	0.500	0.519	0.504
45	0.515	0.505	0.512	0.508	0.516	0.505
90	0.513	0.509	0.525	0.507	0.537	0.532
105	0.517	0.510	0.527	0.504	0.507	0.502
120	0.524	0.512	0.525	0.502	0.520	0.508
135	0.532	0.511	0.519	0.504	0.532	0.511
180	0.522	0.507	0.510	0.500	0.519	0.504

continuously distributed dislocation method. The results are shown in Tables 1 and 2. In general, good agreement is found between the two methods.

The second example is an anisotropic rectangular plate of width $2w$ and height $2h$ with a central crack inclined at 45° to the x-axis (Fig. 5). The plate is loaded by a uniform tension in the y direction. The ratios of crack length to width, and of height to width are a/W=0.2 and h/w=2.0, respectively. The material is glass-epoxy with elastic properties E=48.26 GPa, E'=17.24 GPa, ν'=0.29, and G'=6.89 GPa (Sollero and Aliabadi, 1993). The direction of the fibers was rotated from ψ=0° to ψ=180°. The outer boundary and the crack surface are discretized with 32 continuous and 10 discontinuous quadratic elements, respectively. Table 3 shows the results obtained by this study as well as those by Sollero and Aliabadi (1993) with a sub-regional BEM, and Gandhi (1972) with a mapping collocation technique. Again, excellent agreement is obtained.

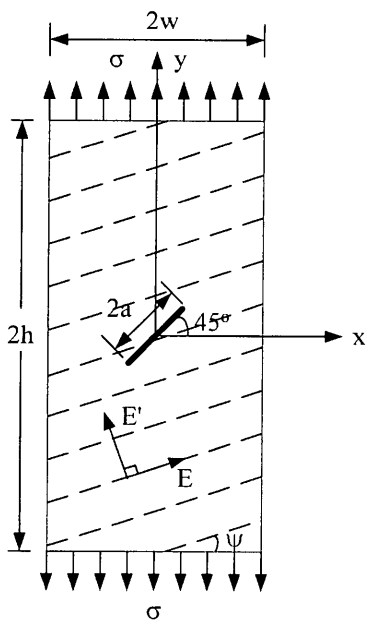

Fig. 5. An anisotropic rectangular plate with a central crack inclined 45° under uniform tension.

IV. CRACK INITIATION AND FRACTURE PROPAGATION

In order to check the validity of our crack initiation prediction procedure, the tests of Erdogan and Sih (1963) were reproduced numerically with our BEM formulation. Erdogan and Sih conducted

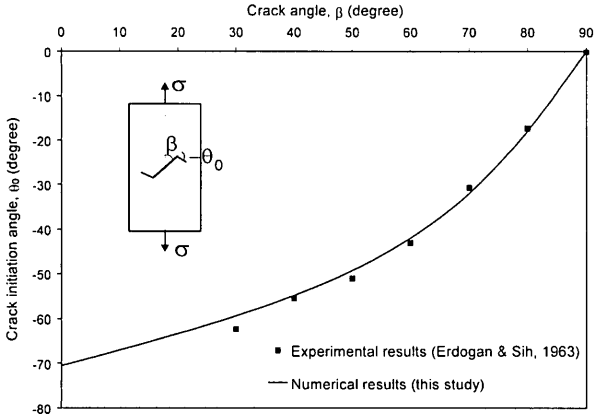

Fig. 6. Variation of crack initiation angle θ_0 with the crack angle β. Plexiglass plate subjected to uniaxial tension.

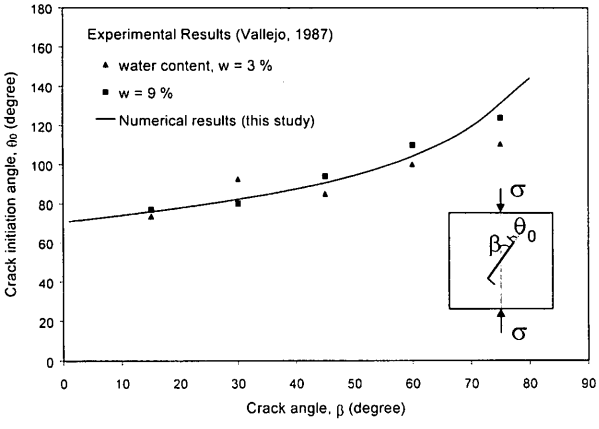

Fig. 7. Variation of crack initiation angle θ_0 with the crack angle β. Prismatic sample of kaolinite clay subjected to uniaxial compression.

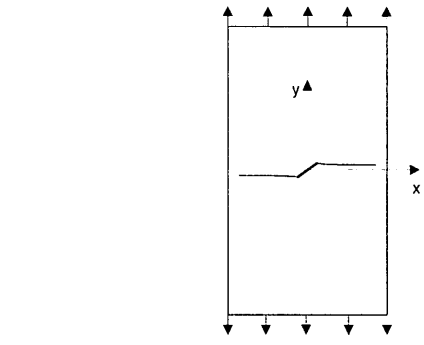

(a)

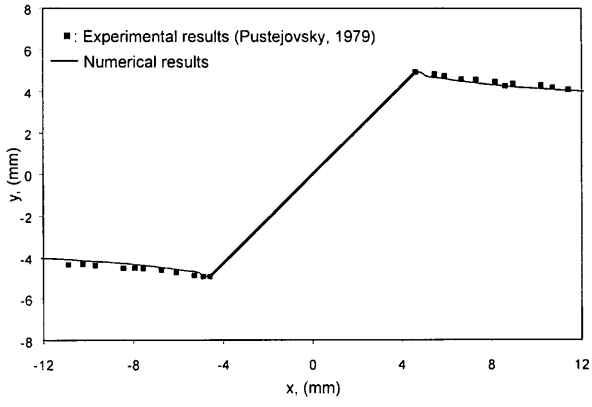

(b)

Fig. 8. (a) Numerical siumlation of crack propagation (β=43°). Plate of titanium subjected to uniaxial tension. (b) Comparison of simulated crack propagation with experimental observation of a titanium plate in the vicinity of the crack tips.

uniaxial tension tests on isotropic Plexiglass sheets 229×457×4.8 mm in size containing a 50.8 mm long central crack. The crack orientation angle β between the crack plane and the tensile stress was varied. Fig. 6 shows the variation of the crack initiation angle θ_0 with the crack angle β determined numerically and experimentally. A good agreement is found between the experimental results of Erdogan and Sih (1963) and our numerical predictions.

Another verification was done using the experimental results of Vallejo (1987). The latter conducted uniaxial compression tests on cracked prismatic specimens of kaolonite clay 76.2×76.2×25.4 mm in size containing a central crack 24.9 mm in length. Several tests were carried out by varying the crack angle β between the crack plane and the compressive stress. Fig. 7 shows a comparison between the crack initiation angles measured experimentally and those predicted numerically. Again, a good agreement is found between the two approaches.

Comparison of fracture propagation simulation by the proposed BEM with the experimental results is discussed in the following. Pustejovsky (1979) conducted a series of uniaxial tension tests on isotropic titanium Ti-6Al-4V plates with a central inclined crack. The reported material properties of the specimens were E=112 GPa, ν=0.29, and the ultimate tensile strength T_u=945 MPa. The specimens were 76.2×203.2×3.2 mm in size and were cut using a carbide cutoff-wheel to give a initial crack length $2a$= 13.5 mm. One of the test specimens (defined as the CSG-04 specimen) had a crack angle β=43°. A numerical simulation of crack propagation in that specimen was conducted with the BEM using 32 continuous quadratic elements for the outer boundary and 10 discontinuous elements for the crack boundary. The result of the numerical simulation is shown in Fig. 8(a). It is noted that the subsequent crack path is slightly curved and nearly perpendicular to the applied load. This observation is consistent with the results of Yan and Nguyen-Dang (1995) using the Dual BEM. Comparison of simulated crack propagation with the experimental observations of Pustejovsky (1979) in the vicinity of the crack tip is

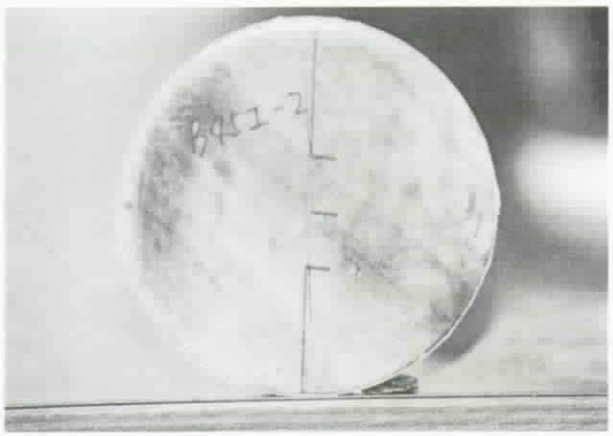

(a)

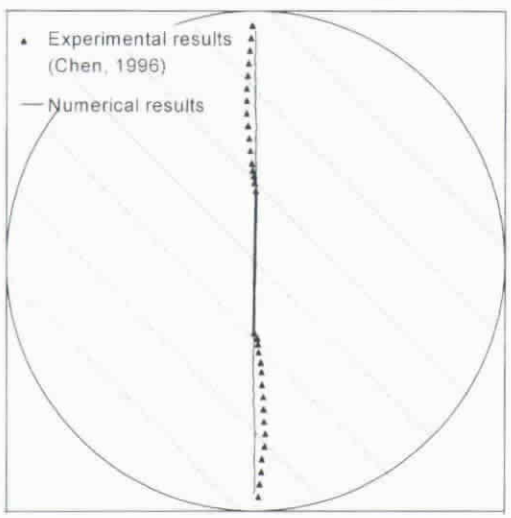

(b)

Fig. 9. (a) Photograph of specimen SB1-2 after failure (ψ=45°, β=0.8°). (b) Propagation of a crack at the center of a circular plate of oil shale under concentrated diametrical loading. Comparison between experimental observations and numerical predictions for specimen SB1-2 with ψ=45° and β=0.8°.

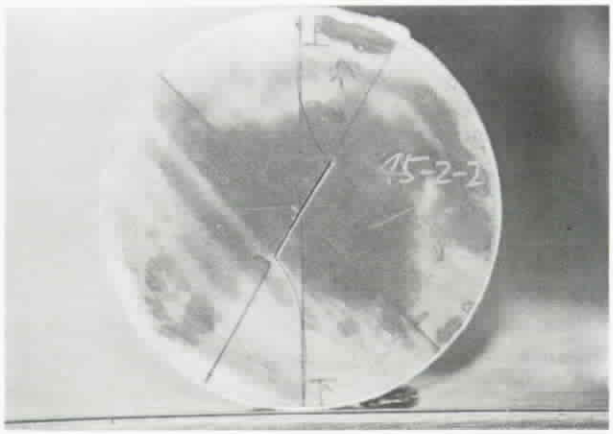

(a)

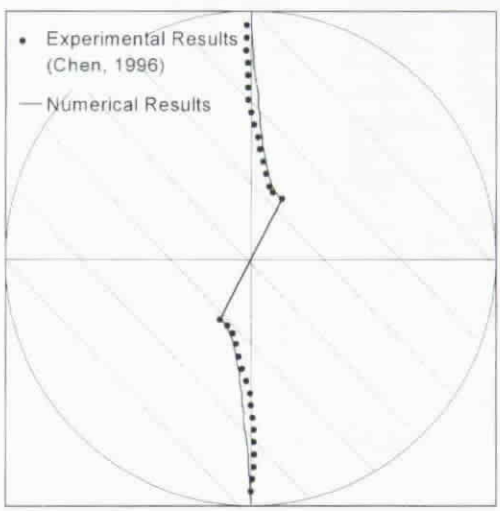

(b)

Fig. 10. (a) Photograph of specimen SB2-2 after failure (ψ=45° and β=27.6°). (b) Propagation of a crack at the center of a circular plate of oil shale under concentrated diametrical loading. Comparison between experimental observations and numerical predictions for specimen SB2-2 with ψ=45° and β=27.6°.

shown in Fig. 8(b). A good agreement is found between the experimental results and the numerical prediction.

In order to verify further the validity of the proposed BEM procedure to predict fracture propagation in anisotropic materials, the propagation path in a central cracked circular plate of oil shale was numerically predicted and compared with the actual laboratory observations (Chen, 1996). In these experiments, a crack initially inclined with respect to the applied stress was allowed to grow under concentrated diametrical loading. Chen (1996) conducted the Brazilian tests (Fig. 4) on initially cracked circular specimens with a diameter of 7.0 cm, a thickness of 0.9 cm, and a crack length of 1.95 cm. The elastic properties of the bedding oil shale were E=1.43 GPa, E'=1.17 GPa, ν=0.462, ν'=0.339, and G'=0.47 GPa. Details of specimen dimension, testing procedure, and crack geometry can be found in Chen (1996). Two of the test specimens with the same material inclination angle ψ=45°, defined as the SB1-2 and SB2-2, had crack angle β=0.8° and 27.6°, respectively. Photographs showing specimens SB1-2 and SB2-2 after failure and the crack propagation paths are shown in Figs. 9(a) and 10(a), respectively. All crack propagation paths tend to be parallel to the loading direction and to approach the loading points. The BEM was also used to simulate fracture propagation in these oil shale specimens. The outer boundary and crack surface were discretized with 28 continuous and 20 discontinuous quadratic elements, respectively. Figs 9(b) and 10(b) show the observed and predicted

fracture propagation paths for specimens SB1-2 and SB2-2, respectively. Good agreement is found between the two approaches. It is therefore concluded that the proposed BEM procedure can simulate well the process of fracture propagation for both isotropic and anisotropic plates.

V. CONCLUSIONS

This paper shows that the mixed mode SIF's of anisotropic plate can be successful determined by the proposed BEM. Numerical examples of the calculation of SIF's for both isotropic and anisotropic plates were conducted and good agreement with previously published results was obtained. A new BEM procedure based on the maximum tensile stress failure criterion was developed to predict the crack initiation direction and the fracture propagation path in anisotropic plates under mixed mode loading. A good agreement was found between crack initiation and propagation predicted with the proposed BEM and experimental observations reported by previous researchers on both isotropic and anisotropic materials.

NOMENCLATURE

σ, τ	normal and shear stresses (F/L^2)
β	crack orientation angle (degree)
ψ	material inclination angle (degree)
ν	Poisson's ratio
ρ	ratio of stress intensity factor
λ	ratio of the relative crack-tip displacements
Γ_B, Γ_C	outer boundary and crack boundary
$2a$	crack length (L)
E, G	Young's modulus and shear modulus of material (F/L^2)
K_I, K_{II}	stress intensity factors for mode I and II ($F/L^{3/2}$)
T_{ij}, U_{ij}	the Green's tractions and displacements (F/L^2, L)
u, v	displacements in the x- and y-directions (L)

REFERENCES

1. Aliabadi, M.H., 1997, "Boundary Element Formulation in Fracture Mechanics," *Applied Mechanics Review*, Vol. 50, pp. 83-96.
2. Atkinson, C., Smelser R.E., and Sanchez, J., 1982, "Combined mode fracture via the cracked Brazilian disk test," *International Journal of Fracture*, Vol. 18, No. 4, pp. 279-291.
3. Blandford, G.E., Ingraffea, A.R., and Liggett, J.A., 1981, "Two-dimensional stress intensity factor computations using the boundary element method," *International Journal for Numerical Methods in Engineering*, Vol. 17, pp. 387-404.
4. Boone, T.J., Wawrzynek, P.A., and Ingraffea, A. R., 1987, "Finite Element Modelling of Fracture Propagation in Orthotropic Materials," *Engineering Fracture Mechanics*, Vol. 26, No. 2, pp. 185-201 (1987).
5. Cerrolaza, M., and Alarcon, E., 1989, "A bi-cubic Transformation for the Numerical Evaluation of the Cauchy Principal Value Integrals in Boundary Methods," *International Journal for Numerical Methods in Engineering*, Vol. 28, pp. 987-999.
6. Chen, C.S., 1996, "Characterization of Deformability, Strength and Fracturing of Anisotropic Rocks Using Brazilian Tests," Ph.D. Thesis, Department of Civil Engineering, University of Colorado, Boulder.
7. Chen, C.S., Pan, E., and Amadei, B., 1998, "Determination of Deformability and Tensile Strength of Anisotropic Rocks Using Brazilian tests," *International Journal of Rock Mechanics and Mining Sciences & Geomechanics Abstracts*, Vol. 35, No.1, pp. 43-61.
8. Chen, J.T., and Hong, H.K., 1992, "Boundary Element Method," *New World Publication* Com., Taiwan, R.O.C. (in Chinese)
9. Chen, J.T., and Hong, H.K., 1999, "Review of Dual Boundary Element Methods with Emphasis on Hypersingular Integrals and Divergent Series," *Applied Mechanics Review, ASME*, Vol. 52, No. 1, pp. 17-33.
10. Crouch, S.L., and Starfield, A.M., 1983, "Boundary Element Methods in Soild Mechanics," *George Allen and Unwin Publishers*, London.
11. Erdogan, F., and Sih, G.C., 1963, "On the Crack Extension in Plates Under Plane Loading and Transverse Shear," *Journal of Basic Engineering*, Vol. 85, pp. 519-527 .
12. Gandhi, K.R., 1972, "Analysis of an Inclined Crack Centrally Placed in an Orthotropic Rectangular Plate," *Journal of Strain Analysis*, Vol. 7, pp. 157-162.
13. Gray, L.J., Martha, L.F., and Ingraffea, A.R., 1990, "Hypersingular Integrals in Boundary Element Fracture Analysis," *International Journal for Numerical Methods in Engineering*, Vol. 29, pp. 1135-1158.
14. Griffith, A.A., 1920, "The Phenomena of Rupture and Flow in Solids," *Philosophical Transactions of the Royal Society of London*, Series A, Vol. 221, pp. 163-198.
15. Hildenbrand, J., and Kuhn, G., 1993, "Non-linear Co-ordinate Transformation of Finite Part Integrals in Two-dimensional Boundary Element Analysis", *International Journal for Numerical Methods in Engineering*, Vol. 36, pp. 2939-2954.

16. Hong, H.K., and Chen, J.T., 1988, "Derivations of Integral Equations of Elasticity," *Journal of Engineering Mechanics*, Vol. 114, pp. 1028-1044.
17. Irwin, G.R., 1957, "Analysis of Stresses and Strains Near the End of a Crack," *Journal of Applied Mechanics*, Vol. 24, pp. 361-364.
18. Lekhnitskii, S.G., 1957, "Anisotropic plates," *translated by S.W. Tsai*, Gordon and Breath.
19. Linkov, A.M., and Mogilevskaya, S.G., 1994, "Complex Hypersingular Integrals and Integral Equations in Plane Elasticity," *Acta Mechanica*, Vol. 105, pp. 189-205.
20. Palaniswamy, K., and Knauss, W.G., 1972, "Propagation of a Crack Under General, In-plane Tension," *International Journal of Fracture*, Vol. 8, pp. 114-117.
21. Pan, E., and Amadei, B., 1996, "Fracture Mechanics aAnalysis of 2-D Anisotropic Media with a New Formulation of the Boundary Element Method," *Interational Journal of Fracture*, Vol. 77, pp. 161-174.
22. Pan, E., 1997, "A General Boundary Element Analysis of 2-D Linear Elastic Fracture Mechanics," *International Journal of Fracture*, Vol. 88, pp. 41-59.
23. Portela, A., Aliabadi, M.H., and Rooke, D.P., 1993, "Dual Boundary Element Incremental Analysis of Crack Propagation," *Computers and Structures*, Vol. 46, No. 2, pp. 237-247.
24. Portela, A., Aliabadi, M.H., and Rooke,D.P., 1992, "The Dual Boundary Element Method: Effective Implementation for Crack Problems," *International Journal for Numerical Methods in Engineering*, Vol. 33, pp. 1269-1287.
25. Pustejovsky, M.A., 1979, "Fatigue Crack Propagation in Titanium Under General In-plane Loading - I: Experiments," *Engineering Fracture Mechanics*, Vol. 11, pp. 9-15.
26. Richard, H.A., 1984, "Examination of Brittle Fracture Criteria for Overlapping Mode I and Mode II Loading Applied to Cracks," In *Application of Fracture Mechanics to Materials and Structures*, ed. G.C. Sih *et al.*, Martinus Nijhoff Pub., pp. 309-316.
27. Scavia, C., 1995, "A Method for the Study of Crack Propagation in Rock Structures," *Geotechnique*, Vol. 45, No. 3, pp. 447-463.
28. Shen, B., and Stephansson, O., 1994, "Modification of the G-criterion for Crack Propagation Subjected to Compression," *Engineering Fracture Mechanics*, Vol. 47, No. 2, pp. 177-189.
29. Shephard, M.S., Yehia, N.A.B., Burd, G.S., and Weidner, T.J., 1985, "Automatic Crack Propagation Traction," *Computers and Structures*, Vol. 20, pp. 211-223.
30. Sih, G.C., 1974, "Strain-energy Density Factor Applied to Mixed Mode Crack Problems," *International Journal of Fracture*, Vol. 10, No. 3, pp. 305-321.
31. Snyder, M.D., and Cruse, T.A., 1975, "Boundary-integral Analysis of Anisotropic Cracked Plate," *International Journal of Fracture*, Vol. 11, pp. 315-328.
32. Sollero, P., and Aliabadi, M.H., 1995, "Anisotropic Analysis of Cracks in Composite Laminates Using the Dual Boundary Element Method," *Composite Structures*, Vol. 31, pp. 229-233.
33. Sollero, P., and Aliabadi, M.H., 1993, "Fracture Mechanics Analysis of Anisotropic Plates by the Boundary Element Method," *International Journal of Fracture*, Vol. 64, pp. 269-284.
34. Sollero, P., Aliabadi, M.H., and Rooke, D.P., 1994, "Anisotropic Analysis of Cracks Emanating from Circular Holes in Composite Laminates Using the Boundary Element Method," *Engineering Fracture Mechanics*, Vol. 49, No. 2, pp. 213-224.
35. Swenson, D.V., and Ingraffea, A.R., 1988, "Modelling Mixed-mode Dynamic Crack Propagation Using Finite Elements: Theory and Applications," *Computational Mechanics*, Vol. 3, pp. 381-397.
36. Tsamasphyros, G., and Dimou, G., 1990, "Gauss Quadrature Rules for Finite Part Integrals," *International Journal for Numerical Methods in Engineering*, Vol. 30, pp. 13-26.
37. Vallejo, L.E., 1987, "The Brittle and Ductile Behavior of a Material Containing a Crack Under Mixed-mode Loading," *Proceedings of the 28th U.S. Symposium on Rock Mechanics*, University of Arizona, Tucson, pp. 383-390.
38. Wawrzynek, P.A., Martha, L.F., and Ingraffea, A.R., 1988, "A Computational Environment for the Simulation of Fracture Processes in Three Dimensions," In *Analysis of Numerical Experiment Aspects of Three-dimensional Fracture Process*, A.J. Rosakis et al. (Eds.), ASME, AMD-91, pp. 321-327.
39. Wei, K., and Bremaecker, J.-C. De, 1994, "Fracture Growth Under Compression," *Journal of Geophysical Research*, Vol. 99, No. B7, pp. 13, 781-13,790.
40. Whittaker, B.N., Singh, R.N., and Sun, G., 1992, "Rock Fracture Mechanics: Principles, Design and Applications," *Elsevier*, New York.
41. Woo, C.W., and Ling, H.L., 1984, "On Angle Crack Initiation Under Biaxial Loading," *Journal of Strain Analysis*, Vol. 19, No. 1, pp. 51-59.
42. Yan, A.M., and Nguyen-Dang, H., 1995, "Multiple-cracked Fatigue Crack Growth by BEM," *Computational Mechanics*, Vol. 16, pp. 273-280.

Discussions of this paper may appear in the discussion section of a future issue. All discussions should be submitted to the Editor-in-Chief.

Manuscript Received: May 20, 1999
Revision Received: June 18, 1999
and Accepted: July 30, 1999

利用邊界元素法探討異向性薄板之裂縫傳播行爲

陳昭旭　柯建仲

國立成功大學資源工程學系

摘　要

本文提出一邊界元素法結合最大張應力破壞準則，針對一具有裂縫之異向性薄板承受載重，來預測其裂縫初始成長角度，並模擬其裂縫傳播路徑。首先利用邊界元素法與J積分技術可成功求出裂縫尖端之應力強度因子，經由此些因子可進一步計算出裂縫初始成長角度，根據此角度增加一微小線型元素，如此反覆運算可用以模擬裂縫成長過程。經與前人研究之實驗結果比較，發現本文所提之邊界元素法過程，可成功模擬異向性薄板之裂縫傳播路徑。

關鍵詞：邊界元素法、應力強度因子、裂縫傳播、異向性薄板